Journal of Medical Ultrasonics (2019) 46:287–296
https://doi.org/10.1007/s10396-019-00930-w

ORIGINAL ARTICLE

Fast adaptive beamforming through a cascade structure for ultrasound imaging

Seyede Elham Shamsian[1] · **Sayed Mahmoud Sakhaei**[1]

Received: 13 October 2018 / Accepted: 10 January 2019 / Published online: 22 February 2019

Abstract

Purpose A major limiting factor for applying a minimum variance (MV) beamformer in medical ultrasound imaging is its high computational complexity. This paper introduces a new fast MV beamforming method with almost the same capabilities as the standard MV.

Methods The fast beamformer is implemented using a cascade structure. At the first stage, the echo signals received from the points far from the main axis are strongly suppressed using a fixed-weight beamformer. At the second stage, after spatially decimating the output of the first stage, an MV-based adaptive beamformer is used to eliminate the echo signals from the points adjacent to the focal point. The greatest advantage of the proposed method is that the second beamformer can be a low-complexity implementation of MV such as beamspace (BS) MV to further reduce the complexity, resulting in a superfast MV.

Results The resulting beamformers were evaluated through both simulation and experimental data, and it was verified that the method was competitive with standard MV and BS methods at a lower computational cost.

Conclusion The new fast and superfast MV methods are capable of obtaining the same results as the MV and BS-MV, at a significantly lower computational cost.

Keywords Adaptive beamforming · Ultrasound imaging · Minimum variance · Computational complexity · Beamspace

Introduction

Minimum variance (MV) beamformers have mostly been studied for ultrasound imaging [1–8]. In the MV method, the power of the signal at the beamformer output is minimized while retaining the desired signal. This method is capable of suppressing the strong off-axis signals, and consequently the resolution is significantly enhanced. This improvement comes at a cost: whereas the computational complexity of a Delay And Sum (DAS) beamformer is linear in the number of elements [O(M)], that of MV is up to $O(M^3)$ due to the inversion of the spatial covariance matrix. Therefore, the computational complexity is a major drawback of the MV.

The problem of MV beamforming in the beamspace (BS) domain was investigated by Nilsen et al. [9], who proposed an approximate method for implementing the MV. The authors showed that the number of beams used for the beamforming process can be much lower than the array length, while attaining a resolution comparable to that of MV. In this way, the computational complexity of the beamformer is almost reduced to the order of $O(M^2)$, provided that the number of beams is much smaller than M. Instead of DFT used in their study [9], discrete cosine transform (DCT) [10] and Legendre polynomial expansions [11] have also been used for reducing the complexity of adaptive beamforming. Furthermore, another dimension reduction-based method was established on principal components of the covariance matrix [12].

In a study by Asl and Mahloojifar [13], by approximating the estimated covariance matrix as a Toeplitz matrix, the computational complexity was decreased to $O(M^2)$. A fast method for calculating MV output through $O(M^2)$ computations was addressed in a report by Park et al. [14]. However, this method applies no approximations, but its advantage is lost when temporal averaging or diagonal loading is applied. A low-complexity adaptive (LCA) beamformer was proposed by Synnevag et al. [15]. This method applies several predefined windows on the received signals and determines the best window according to the MV criterion. While the

✉ Sayed Mahmoud Sakhaei
smsakhaei@nit.ac.ir

[1] Department of Electrical and Computer engineering, Babol Noshirvani University of Technology, Babol, Iran

computational complexity of this method is linear [O(M)], the image may represent amplitude fluctuations not really present in the medium, as a result of the discrete solution space used.

A decimated MV (DMV) beamformer with linear complexity was described by Sakhaei [16]. DMV is established on the assumption that the interferences mainly originate from the scatterers near the point to be imaged. This assumption is especially valid in focused wave imaging. The method provides significant improvement in image resolution compared with other linear complexity beamformers such as DAS and LCA.

In this paper, we exploit the idea of Sakhaei [16] for complexity reduction, which is the decimation of the aperture, and extend the idea to introduce a new implementation of the MV with a comparable resolution and contrast to the standard MV, but at a lower computational complexity. In the fast method suggested here, the interference signals received by the array are suppressed at two consecutive stages using two different beamforming methods: a fixed beamformer to choose the sub-beam of interest, followed by an adaptive one applied on the spatially decimated data. Hence, we call the new method a decimated sub-beam MV (DSMV) beamformer. To achieve greater reduction in the computational burden, we suggest that the second-stage beamformer be implemented using a low-complexity method such as those described in other reports [9–14]. Using the BS method instead of MV beamforming at the second stage of the DSMV beamformer, we obtain a superfast beamformer referred to DSBS, the results of which are very similar to those obtained by the one-stage BS beamformer described by Nilsen et al. [9].

This paper is organized as follows. The background material is presented in the next section, including the MV beamformer and the methods for estimating and regularizing the covariance matrix. The third section describes the DSMV and DSBS methods. The simulation results for validating the proposed method are described in the fourth section, and the obtained experimental results are illustrated in the fifth section, followed by a section discussing some characteristics of the proposed method. Finally, the conclusions are given in the last section.

Minimum variance beamformer

Consider a linear array transducer in the receiving mode consisting of M elements, where $x_m[n]$ is the pre-steered sample output from element m at time n. The output of the beamformer is given by

$$y[n] = \vec{w}[n]^H \vec{x}[n]. \tag{1}$$

With

$$\vec{x}[n] = \left[x_1[n], x_2[n], \ldots, x_M[n]\right]^T \tag{2}$$

and

$$\vec{w}[n] = \left[w_1^*[n], w_2^*[n], \ldots, w_M^*[n]\right]^T, \tag{3}$$

$w_m^*[n]$ is the weight applied to the m'th element on the array. The superscripts T, *, and H denote the transpose, complex conjugate, and conjugate transpose operators, respectively.

The MV beamformer finds the optimal apodization weights by minimizing the output power while maintaining a unit gain in the desired signal [1]:

$$\begin{aligned} &\min E\left[|y[n]|^2\right] = \min \vec{w}[n]^H R[n] \vec{w}[n] \\ &\text{subject to : } \vec{w}[n]^H \vec{a} = 1 \end{aligned}, \tag{4}$$

where $R[n] = E\left[\vec{x}[n]\vec{x}[n]^H\right]$ is the spatial covariance matrix and $\vec{a}$ is the steering vector. Based on the assumption of dynamic focus on reception, the steering vector simply becomes a vector of ones [1]. The solution to the minimization problem in Eq (4) is [1]

$$\vec{w}[n] = \frac{R[n]^{-1}\vec{a}}{\vec{a}^H R[n]^{-1}\vec{a}}. \tag{5}$$

In medical ultrasound imaging, the covariance matrix is estimated through a spatial smoothing technique [3–5, 17]. In this technique, the array is divided into $P = M - L + 1$ overlapping subarrays, where $L < M/2$ is the subarray length. The covariance matrix is calculated for each subarray and finally averaged:

$$\hat{R}[n] = \frac{1}{P}\sum_{p=1}^{P} \vec{x}_p[n]\vec{x}_p^H[n], \tag{6}$$

where $\vec{x}_p[n]$ is a vector containing the data at p'th subarray:

$$\vec{x}_p[n] = \left[x_p[n], x_{p+1}[n], \ldots, x_{p+L-1}[n]\right]^T, \quad p = 1, 2, \ldots, P. \tag{7}$$

To get an image with speckle statistics similar to those of DAS, temporal averaging is used. In this technique, the spatially smoothed covariance matrix is averaged over $2K + 1$ temporal samples, where K is such that the length of the temporal samples is not greater than the length of the excitation pulse [18]. Therefore, the estimated covariance matrix through spatial smoothing and temporal averaging is given by

$$\hat{R}[n] = \frac{1}{(2K+1)P}\sum_{k=-K}^{K}\sum_{p=1}^{P} \vec{x}_p[n-k]\vec{x}_p^H[n-k]. \tag{8}$$

Using the estimation of the covariance matrix, the MV optimum weights are calculated through Eq. (6), and then the final MV beamformed output is given by

$$y[n] = \frac{1}{P}\sum_{p=1}^{P} \vec{w}[n]^H \vec{x}_p[n]. \tag{9}$$

To enhance the robustness of the MV beamformer against modeling errors, a diagonal loading technique is used, in which a small positive value is added to all the diagonal elements of

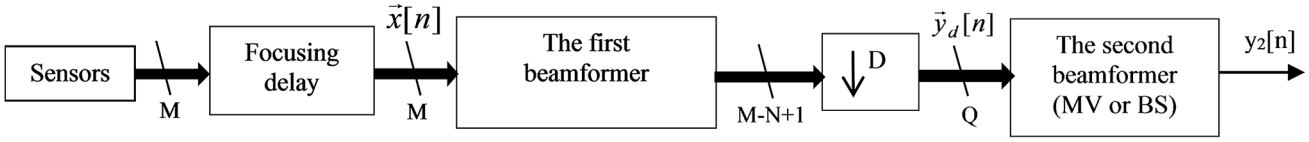

Fig. 1 Diagram of the DSMV (or DSBS) beamformer. The focusing delay box is for dynamic receive focusing. The first beamformer applies a spatial low-pass filter to suppress interferences from points far from the main axis, and then decimation is applied through a box denoted by D, where the dimension of the output is D-times lower than that of the input: $Q = (M - N + 1)/D$. The final output is formed by applying the MV (or BS) beamformer

the estimated covariance matrix [3]. By this technique, $\hat{R}[n]$ is replaced by $\hat{R}[n] + \varepsilon I$, where ε is usually calculated by

$$\varepsilon = \Delta.tr\{R[n]\}, \tag{10}$$

and Δ, the diagonal loading factor, is a constant, and $\mathrm{tr}\{\cdot\}$ is the trace operator.

Proposed methods

Our first proposed method is referred to as the decimated sub-beam minimum variance (DSMV) beamformer, which implements an MV-like beamformer at two consecutive stages. At the first stage, the echo signals received from points laterally far from the main axis are effectively suppressed using a beamformer with predefined fixed weights. This means that a beampattern with a small sidelobe level is desirable for the first stage. On the other hand, the role of this stage is not to suppress the interferences near the main axis, meaning that it is not required to have a narrow mainlobe. Therefore, the first-stage beamformer can be implemented by a small-length array.

The function of this stage can also be clarified in the spatial Fourier transform domain, assuming a continuous-wave (CW) mode. The spatial Fourier transform of the signal received by array elements can be used to describe the spatial distribution of the wave arriving at the array: low-frequency components represent the wave received from scatterers at the focal region, and high-frequency components demonstrate the wave received from those far from the focal point [19, 20]. Therefore, the echo signals received from the scatterers far from the main axis could be eliminated by applying a spatial low-pass filter on the signal received by the array. In this way, the beamformer at the second stage deals with eliminating the interference signals generated by scatterers close to the focal point. As the strong interferences usually originate from the scatterers close to the focal point, a high-resolution beamformer such as MV is an effective choice for the second stage. Finally, in a beamspace view, the first beamformer acts as a processor on the central beam and neglects other beams.

At the output of the first stage, the signals are obtained through a spatial low-pass filter. This filter acts as an anti-aliasing spatial filter, and hence the output can be spatially decimated by a factor whose value is inversely dependent in the mainlobe width of the beampattern: narrower mainlobe width permits a higher decimation factor. This channel reduction results in a lowered computational complexity for implementing MV at the second stage, while preserving the array length. This means that the decimation will not affect the system resolution. Figure 1 summarizes the procedure for applying the DSMV beamformer in a diagram.

If J is the length of the filter (or beamformer) at the first stage with weight vector $\vec{f}$ of size J, then the first-stage output is given by

$$\vec{y}_1[n] = X_1^T[n]\vec{f}, \tag{11}$$

where $X_1[n]$ is a $J \times (M - J + 1)$ matrix defined as follows:

$$X_1[n] = \left[\vec{x}_1[n], \vec{x}_2[n], \ldots, \vec{x}_{M-J+1}[n]\right]. \tag{12}$$

After data decimation, $\vec{y}_1[n]$ is collapsed to a $Q \times 1$ vector $\vec{y}_d[n]$, where Q is the nearest integer not greater than $(M - J + 1)/D$ and D is the decimation factor:

$$y_{d,i}[n] = y_{1,iD}[n], \tag{13}$$

which indicates that the ith element of $\vec{y}_d$ is equal to the iDth element of $\vec{y}_1$. To apply the MV beamformer on $\vec{y}_d[n]$, the covariance matrix is estimated using the spatial smoothing on $\mathrm{P} = Q - L + 1$ overlapping subarrays each with length L along with the temporal averaging technique represented in Eq. (9). The final output of the DSMV beamformer is given by

$$y_2[n] = \frac{1}{P}\sum_{p=1}^{P} \vec{w}_d[n]^H \vec{y}_{dp}[n], \tag{14}$$

where $\vec{y}_{dp} = \left[y_{d,p}, y_{d,p+1}, \ldots, y_{d,p+L-1}\right]^T$ is the data vector at pth subarray, and $\vec{w}_d[n]$ is the MV weight vector calculated for the array data of $\vec{y}_d[n]$. As the length of $\vec{y}_d[n]$ is significantly smaller than the length of the primary array data $\vec{x}[n]$, the computational complexity of DSMV would be seriously lower than that of MV.

Further reduction in complexity can be achieved by implementing the second-stage beamformer through a low-complexity MV such as the BS method. Therefore, we introduce a superfast adaptive beamforming method we call DSBS, which is DSMV with the BS method, at the second

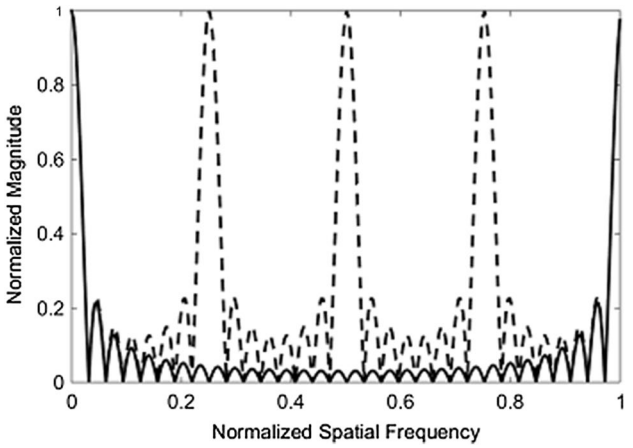

Fig. 2 Beampattern of a 32-element $\lambda/2$-spaced array (solid line), and that of the same array spatially decimated by a factor of 4 (dash line)

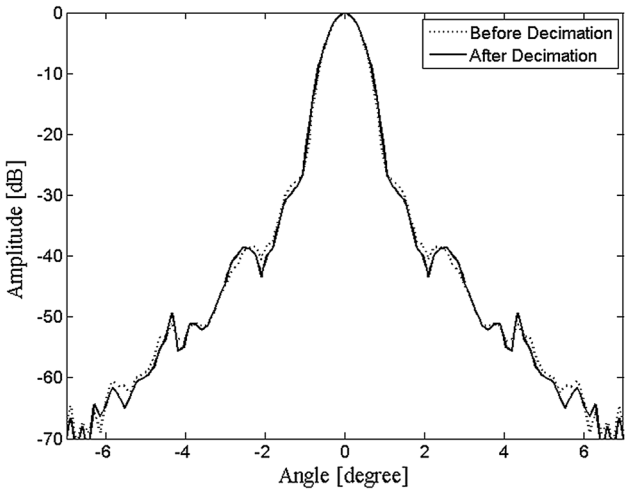

Fig. 3 Beamformed response of the first stage of the DSMV beamformer (rectangular filter, $J=8$, $D=4$), before and after decimation

stage. In other words, the DSBS beamformer processes the received data, respectively, through spatial low-pass filtering, decimating, and then applying beamspace MV beamforming.

Clearly, the key to the reduced complexity of DSMV is the decimation factor D. Large values of D result in a lower complexity, but it might cause an aliasing effect, and a large value of interference power could leak through grating lobes. One way to properly determine D is explained in the following subsection.

Determining the decimation factor

Decimating the data causes additional lobes to appear in the beampattern with the same amplitude as that of the mainlobe. These lobes, referred to as grating lobes, are illustrated in Fig. 2, where the CW beampattern of a 32-element λ/2-spaced array and its decimated one (by a factor of 4) are displayed. The horizontal axis represents normalized spatial frequency, where $u = \pi \sin\theta$ is the spatial frequency versus the looking angle θ, and its normalized value is u/π.

As can be seen from Fig. 2, the first grating lobe appears at a normalized spatial frequency of $\pi/D = 0.25$. If the decimation factor D is such that the power leaking through the grating lobes compared to the total power is negligible, e.g., it is 5% of the total power, it may be calculated as:

$$D_{\max} = \frac{\pi}{u_0}, \tag{15}$$

where u_0 is the spatial frequency above which the power of the beampattern is negligible.

This is a difficult method to calculate D, and an approximate one with easy calculations may be more desirable. To this end, u_0 is approximated as the frequency of the first null of the beampattern, which can be calculated theoretically through the Fourier transform of the weighting function. When a rectangular weighting of length J is used in the first-stage beamformer, the beampattern is represented as:

$$p(u) = \frac{\sin J(u/2)}{\sin(u/2)}. \tag{16}$$

It is obvious that the nulls occur when u is a nonzero multiple of $2\pi/J$. Therefore, the location of the first null is given by

$$u_N = \frac{2\pi}{J}. \tag{17}$$

For example, when the first-stage beamformer is implemented by an array of length $J=8$ elements with rectangular weighting, the first null of its beampattern will be at a spatial frequency of $u = \pi/4$ calculated through Eq (17), and then according to Eq (15), the proper decimation factor will be $D = 4$. Figure 3 illustrates lateral variations of the beamformed responses before and after the decimation for the same array described in the first paragraph of this subsection. It can be concluded from Fig. 3 that by choosing D according to Eqs (15) and (17), the point response of DSMV is almost the same as MV.

Computational complexity

As mentioned earlier, the primary goal of the proposed beamformer is to reduce the computational complexity of MV while preserving the image quality. If we set the length of the filter used at the first-stage beamformer to $J=M/8$, according to Eqs (15) and (17), the decimation factor D will be as follows:

$$D_{\max} = \frac{\pi}{u_N} = \frac{J}{2} = \frac{M}{16}. \tag{18}$$

After the decimation, the input of the second stage will be an array of length $(M-J+1)/D$, which is approximately equal to M/D. As the MV method requires computations in proportion to the third power of the number of array elements ($O(M^3)$), the computation complexity of the new method is approximately D^3 times lower than that of MV ($O(M^3/D^3)$). On the other hand, the complexity of the BS method is $O(M^2)$, and hence that of DSBS is only $O(M^2/D^2)$.

As an example, for $M=64$ and $J=M/8$, we will have from Eq (18): $D=4$, and then the gains in the computational complexity of DSMV and DSBS with respect to MV are 64 and 1024, respectively.

Simulation results

This section describes the array and beamforming parameters, various phantoms used in simulations and the evaluation methods. We then report the results of different beamformers obtained through simulations performed using field II [21].

Simulation setup

The array used in all the simulations was a phased array with $M=64$ elements spaced one-half wavelength apart, a central frequency of 7 MHz, and a sampling frequency of 25 MHz. In all the simulations, fixed focus at a radial distance of 50 mm was used in transmission, and dynamic focus in reception.

In the DAS beamformer, the received signals were summed through rectangular weighting. In the MV beamformer, after applying spatial smoothing with subarray length $L=M/2$ and temporal averaging over $2K+1=21$ samples, the covariance matrix was estimated. Finally, the optimal weights were estimated by the diagonally loaded covariance matrix. For the proposed DSMV beamformer, a uniform apodization filter of length $J=8$ along with the decimation factor $D=4$, calculated by Eq (18) was used in the first-stage beamformer. Hence, the input to the second beamformer was an array signal of length $Q=15$. It was then divided into $P=8$ subarrays each with length $L=8$ to estimate the covariance matrix through spatial smoothing. In the BS beamformer, after the covariance matrix is estimated through the same parameters used in the MV beamformer, the problem is solved in the beamspace domain through three central beams. The parameters of the DSBS beamformer were the same as those used in the DSMV and BS beamformers, i.e., $J=8$, $D=4$, $L=8$, and $N_b=3$. In all the MV-based beamformers, $K=21$ was used for temporal averaging. The diagonal loading factor for MV was $\Delta=1/10L$, and for the other adaptive beamformers, it was chosen such that the beamformed response of a point reflector at a depth of 40 mm was almost the same as that of the MV beamformer. By this examination, Δ was set to $1/20L$ in the BS beamformer, and to $1/30L$ and $1/50L$ in the DSMV and DSBS beamformers, respectively.

Two different phantoms were used for simulation purposes. The first one consisted of 10 point targets placed at depths of 30–70 mm with a lateral distance of 2 mm. It was used for evaluating the resolution of the different beamforming methods. The second phantom was used to compare the contrast of the different beamformers. It was an anechoic cyst with a diameter of 5 mm, centered at a depth of 47.5 mm in a speckle medium.

We evaluated the performance of DSMV and DSBS in comparison to other beamforming methods in terms of resolution, contrast, and robustness. For resolution, two parameters were measured. The first parameter was the -10 dB mainlobe width of a point target (denoted by MLW), and the second one was an indication of the capability of a beamformer to resolve two closely located point targets: the ratio of the peak amplitude to the maximum amplitude occurred in the dip between two point targets (denoted by AR). Lower values of MLW and higher values of AR indicate better resolving capability.

Contrast was evaluated based on the images of the anechoic cyst obtained by different beamforming methods. The contrast ratio (CR) and the contrast-to-noise ratio (CNR) indices were calculated to quantitatively compare the contrast properties of the beamformers. CR is defined as the ratio of the mean value in the background to the mean value in the cyst region [22], and CNR is defined as CR divided by the standard deviation of image intensity in the background region [23].

To compare the robustness of the different beamformers, we considered the uncertainty of sound speed and simulated its effects on the beamformers' outputs. This uncertainty is a result of inhomogeneities of the medium and leads to speed variations. We assumed that the sound speed was constant but known with a 10% overestimation error [3].

Results

In this subsection, we present our results of the two phantoms described in the previous subsection obtained by different beamforming methods.

Figure 4 displays the images of the point target phantom obtained by different beamformers over a 50-dB dynamic range. Figure 5 shows the lateral variations of the beamformed responses at radial distances $r=50$ mm and $r=60$ mm.

As the results show, at both depths, all the MV-based beamformers present narrower mainlobe and lower sidelobe levels, with respect to the DAS. Furthermore,

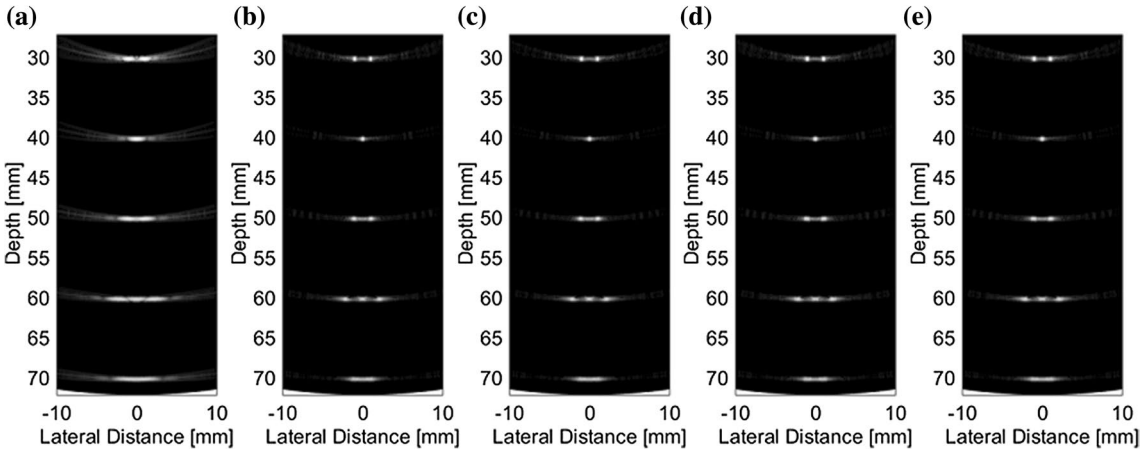

Fig. 4 Images of point-target phantom: **a** DAS (rectangular window); **b** MV ($k=0$, $L=32$); **c** DSMV (rectangular filter, $J=8$, $D=4$, $L=8$); **d** BS ($N_b=3$); and **e** DSBS (rectangular filter, $J=8$, $D=4$, $L=8$, $N_b=3$). The transmit focus is fixed at 50 mm, and the dynamic focus is used in reception

the results obtained by the DSMV and DSBS beamformers are very similar to those obtained by the MV and BS beamformers, respectively. To quantitatively compare the resolution of the different methods, the parameters MLW and AR are calculated for the points at a depth of 60 mm, and the results are given in Table 1. According to the table, the values of AR parameters are almost the same for all MV-based beamformers. Moreover, the values of MLW for MV and DSMV are almost 18% lower than those for BS and DSBS. However, the resolution parameters MLW and AR have no significant changes in MV with respect to DSMV and in BS with respect to DSBS.

To evaluate the contrast properties, we have shown the images of the cyst phantom obtained by the different beamformers in Fig. 6. All the images are displayed with a 50-dB dynamic range. The values of CR and CNR are presented in Table 2 for all the beamformers. As seen, the contrast of the proposed DSMV beamformer is approximately the same as that of the MV in terms of both CR and CNR, and it is much better than those of BS and DSBS. The results also illustrate that the DSBS beamformer gives contrast properties that are only slightly worse than those of the BS beamformer.

For robustness evaluation, we have obtained images of the point-target phantom in the presence of 10% sound speed error. The lateral variations of the responses at a depth of 50 mm are depicted in Fig. 7. It is again seen that the MV and DSMV produce almost the same results. It is also true for the BS beamformer in comparison to the DSBS. Therefore, the robustness of the DSMV and DSBS beamformers against the errors are almost the same as those of the MV and BS beamformers.

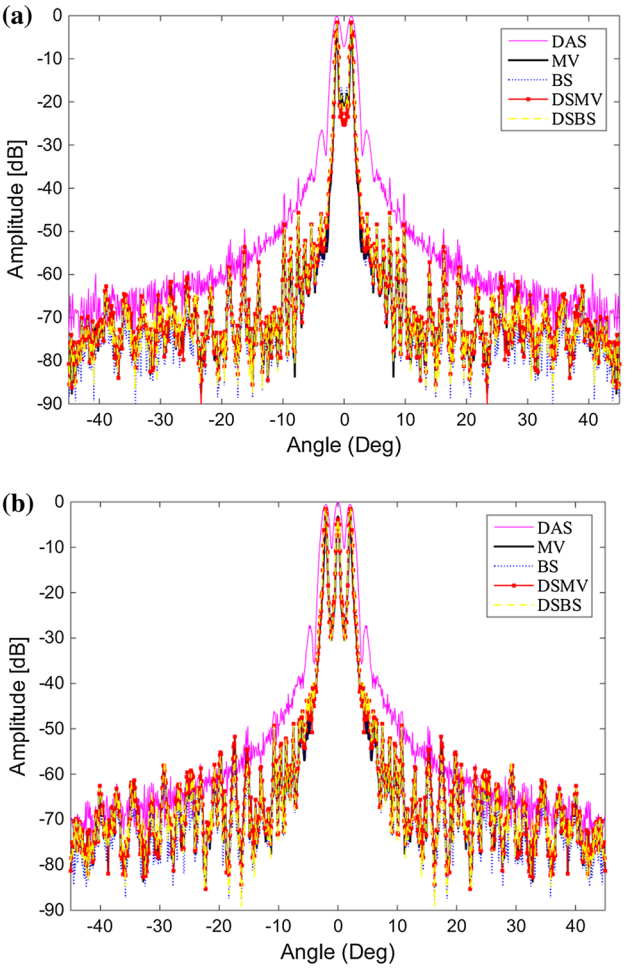

Fig. 5 Beamformed responses of different methods applied to Phantom I at two radial distances: **a** 50 mm and **b** 60 mm

Table 1 Resolution parameters of the response at a depth of 60 mm for different beamformers

	MLW (mm)	AR (dB)
DAS (Delay And Sum)	–	6
MV (Minimum Variance)	0.55	23
DSMV (Decimated Sub-beam MV)	0.57	24
BS (Beamspace MV)	0.66	24
DSBS (Decimated Sub-beam BS)	0.64	24.5

Experimental results

To complete our evaluations of the proposed methods, we applied them to the experimental data of geabr_0[1], which is a complete data set provided by Biomedical Ultrasound Laboratory (BUL) at the University of Michigan. The data are acquired by a 3.33-MHz, 64-element phased array with an element spacing of 0.2413 mm. The echo data were created by a speckle medium containing a combination of wire targets and anechoic cysts. We applied a fixed transmit focus at a radial distance of 70 mm and dynamic receive focusing, and then various beamforming methods were used. For all the MV-based beamformers, 43 samples were used in temporal averaging. All the other parameters of the beamformers were the same as those mentioned in the previous section. The obtained images are displayed in Fig. 8. The lateral variations of the beamformed responses for the center wire and the near anechoic cyst are depicted in Fig. 9. The figures show that all adaptive beamformers provide almost the same resolving capability, which is significantly better than DAS. Moreover, the adaptive beamformers provide darker cysts.

Discussion

As mentioned in introduction, decimation is the process common in DMV and the new method, but there are distinct differences between them. The objective of the DMV is to achieve a beamformer with linear complexity outperforming other linear complexity beamformers such as DAS and LCA, while the DSMV is a method competing with the standard MV method in terms of resolution and contrast at a reduced computational complexity. Correspondingly, the decimation factor in the DSMV is determined such that the aliasing effects are minimized, whereas that in the DMV is such that the capability of the beamformer for imposing proper nulls in the mainlobe of the transmitted field is maintained. Moreover, in the DMV, the filtering process, if applied, is done

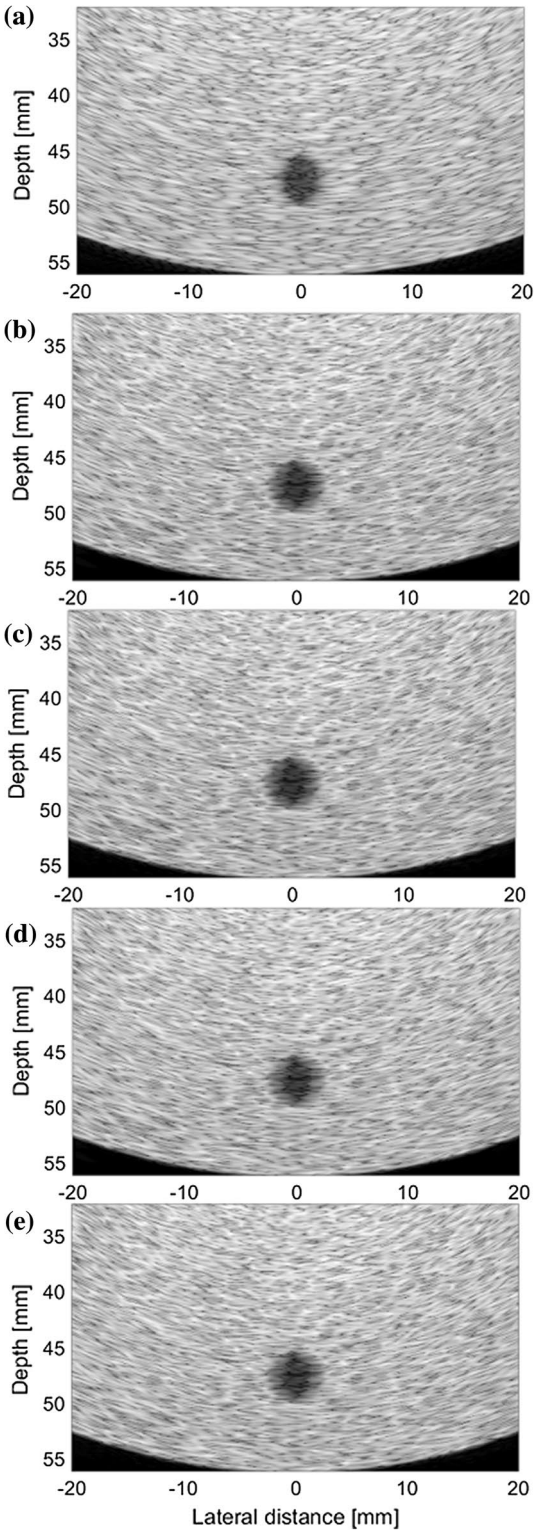

Fig. 6 Simulated cyst phantom images: **a** DAS with uniform weighting; **b** MV with spatial smoothing and temporal averaging; **c** DSMV by applying a rectangular filter ($J=8$, $D=4$, $L=8$); **d** BS ($N_b=3$); and **e** DSBS (rectangular filter, $J=8$, $D=4$, $L=8$, $N_b=3$)

[1] Accessible at http://www.k-space.org/temp/Ultrasound/.

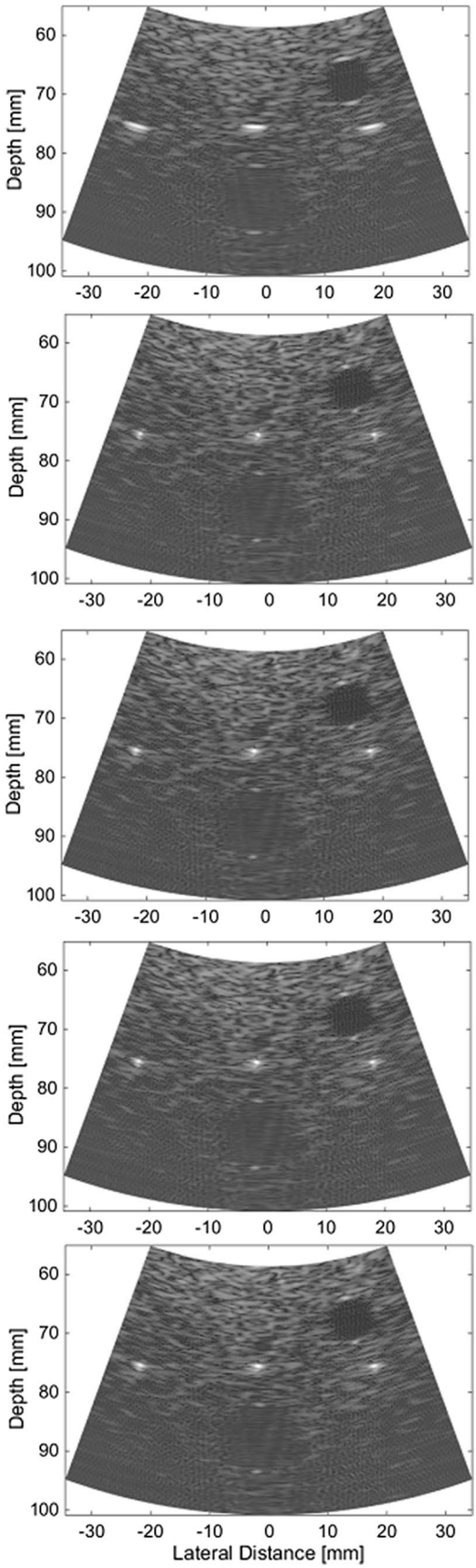

Fig. 8 The reconstructed images from geabr_0 data by different beamforming methods: DAS, MV, DSMV, BS, and DSBS (from top to bottom) ▶

on the subarrays created for spatial averaging. However, in the DSMV, the data on the array are firstly filtered and then divided into subarrays. In this way, the undesired effect of the filtering process on decreasing the apparent array length is mitigated, which results in the enhanced resolving capability of the beamformer.

The diagonal loading technique is an efficient method to enhance the robustness of MV-based beamformers against the errors of wavefield parameters. Moreover, because of applying the first-stage beamformer and also decimating the array, which results in a lowered degree of freedom, the robustness of the DSMV beamformer will be better than that of the MV beamformer with the same diagonal loading factor. Nevertheless, we adjusted the diagonal loading factors such that the MV, DSMV, BS, and DSBS beamformers show a similar response for a point at a depth of 40 mm in the absence of errors. By this selection of diagonal loading, the simulations confirm that the robustness of all adaptive beamformers compared in our study is very similar.

The proposed method applies adaptive beamforming to an array that is decimated by a factor of D. Therefore, as

Table 2 Contrast ratio and contrast-to-noise ratio values for images of a simulated cyst phantom

	I_{bkg} (dB)	I_{cyst} (dB)	CR (dB)	CNR (dB)
DAS	47	25.3	21.7	3.8
MV	47	21.3	25.7	4.4
DSMV	47	21	26	4.4
BS	47.2	23.1	24.1	4.1
DSBS	47.2	22.8	24.4	4.1

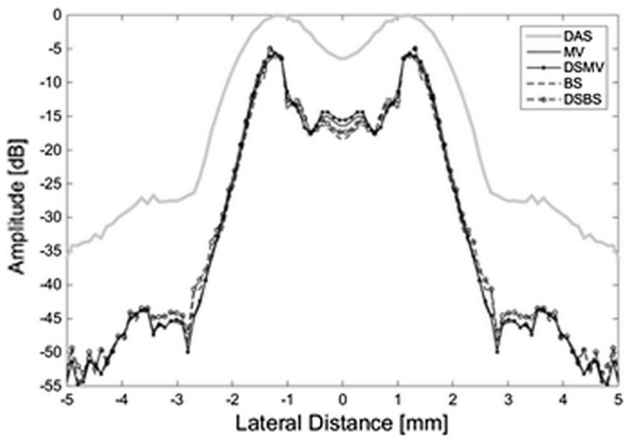

Fig. 7 Beamformed responses of different beamformers at a radial distance of 50 mm in the presence of 10% error on the sound speed estimation

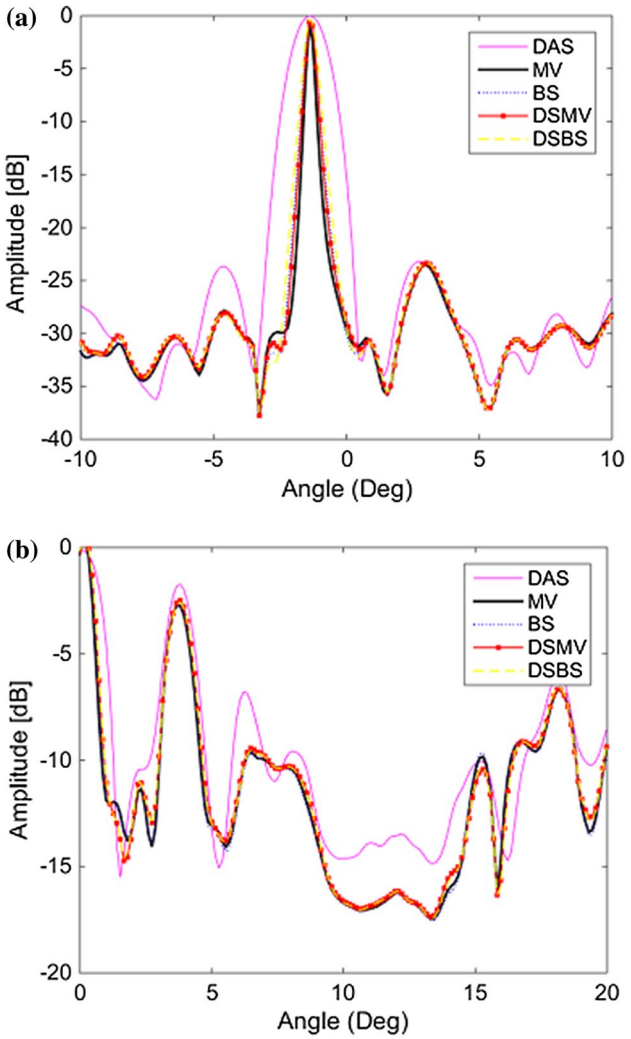

Fig. 9 The lateral variations of the beamformed responses of geabr_0 at a distance of central wire (**a**) and at nearest cyst (**b**)

stated in section III, the computational complexity of the DSMV beamformer is D^3 times smaller than that of the MV. When N_b is small (e.g., $N_b = 3$), the computational complexity of the BS beamformer is dominated by computations needed for calculating the covariance matrix, which is an order of M^2 complexity. Therefore, the complexity of the DSBS beamformer is D^2 times smaller than that of the BS beamformer.

Conclusion

In this paper, we introduced a new fast adaptive beamforming method that simultaneously utilizes two approaches for lowering the computational complexity. The first one is a beamformer called DSMV, in which after applying a fixed beamformer and then spatially decimating the array, MV is used as the final-stage beamformer. The second one is a beamspace MV with a reduced number of beams. The new method, referred to as DSBS, has lower computational complexity in comparison to the BS method. We have also shown that the performance of the DSBS beamformer is very similar to that of the BS method in terms of resolution, contrast, and robustness. Meanwhile, our results confirm that the DSMV beamformer provides better contrast properties than the BS beamformer, while their complexities are almost in the same order.

The main advantage of DSBS over BS is its lower computational complexity. This advantage is greater with larger arrays. Furthermore, it seems that when using an adaptive beamforming method at the first stage instead of using a fixed one, the decimation factor can be lowered at the cost of the complexity of the first-stage beamformer. However, the lower complexity advantage of DSBS over BS may be sustained, especially for large arrays. This is left for future work.

Compliance with ethical standards

Conflict of interest Seyede Elham Shamsian and Sayed Mahmoud Sakhaei declare that they have no conflicts of interest.

Ethical statements This article does not contain any studies with human or animal subjects performed by either of the authors.

References

1. Synnevag JF, Austeng A, Holm S. Adaptive beamforming applied to medical ultrasound imaging. IEEE Trans Ultrason Ferroelectr Freq Control. 2007;54:1606–13.
2. Holfort IK, Gran F, Jensen JA. Broadband minimum variance beamforming for ultrasound imaging. IEEE Trans Ultrason Ferroelectr Freq Control. 2009;56:314–25.
3. Synnevag JF, Austeng A, Holm S. Benefits of minimum-variance beamforming in medical ultrasound imaging. IEEE Trans Ultrason Ferroelectr Freq Control. 2009;56:1868–79.
4. Asl BM, Mahloojifar A. Eigenspace-based minimum variance beamforming applied to medical ultrasound imaging. IEEE Trans Ultrason Ferroelectr Freq Control. 2010;57:2381–90.
5. Mehdizade S, Austeng A, Johansen TF, et al. Eigenspace based minimum variance beamforming applied to ultrasound imaging of acoustically hard tissues. IEEE Trans Med Imaging. 2012;31:1912–21.
6. Hasegawa H. Improvement of penetration of modified amplitude and phase estimation beamformer. J Med Ultrason. 2017;44:3–11.
7. Hasegawa H. Apodized adaptive beamformer. J Med Ultrason. 2017;44:155–65.
8. Sakhaei SM, Shamsian SE. Twofold minimum variance beamforming for enhanced ultrasound imaging. J Med Ultrason. 2018;45:17–24.

9. Nilsen CC, Hafizovic I. Beamspace adaptive beamforming for ultrasound imaging. IEEE Trans Ultrason Ferroelectr Freq Control. 2009;56:2187–97.
10. Deylami AM, Asl BM. A fast and robust beamspace adaptive beamformer for medical ultrasound imaging. IEEE Trans Ultrason Ferroelectr Freq Control. 2017;64:947–58.
11. Bae M, Park SB, Kwon SJ. Legendre polynomial based fast minimum variance beamforming method for medical ultrasound systems. Electron Lett. 2014;50:1570–2.
12. Kim K, Park S, Kim J, et al. A fast minimum variance beamforming method using principal component analysis. IEEE Trans Ultrason Ferroelectr Freq Control. 2014;61:930–45.
13. Asl BM, Mahloojifar A. A low-complexity adaptive beamformer for ultrasound imaging using structured covariance matrix. IEEE Trans Ultrason Ferroelectr Freq Control. 2012;59:660–7.
14. Park J, Wi SM, Lee JS. Computationally efficient adaptive beamformer for ultrasound imaging based on QR decomposition. IEEE Trans Ultrason Ferroelectr Freq Control. 2016;63:256–65.
15. Synnevag JF, Austeng A, Holm S. A low-complexity data-dependent beamformer. IEEE Trans Ultrason Ferroelectr Freq Control. 2011;58:281–9.
16. Sakhaei SM. A decimated minimum variance beamforming for ultrasound imaging. Ultrasonics. 2015;59:119–27.
17. Shan TG, Wax M, Kailath T. On spatial smoothing for direction-of-arrival estimation of coherent signals. IEEE Trans Acoust Speech Signal Process. 1985;33:806–11.
18. Synnevag JF, Austeng A, Holm S. Speckle statistics in adaptive beamforming. In: Proceedings of IEEE Ultrasonics Symposium, 28–31 Oct 2007. IEEE, p. 1545–8.
19. Jeong MK. A Fourier transform-based sidelobe reduction method in ultrasound imaging. IEEE Trans Ultrason Ferroelectr Freq Control. 2000;47:759–63.
20. Naidu PS. Sensor array signal processing. CRC Press; 2009.
21. Jensen JA. Field: a program for simulating ultrasound systems. Med Biol Eng Comput. 1996;34:351–3.
22. O'Donnell M, Flax SW. Phase-aberration correction using signal from point reflectors and diffuse scatterers: measurements. IEEE Trans Ultrason Ferroelectr Freq Control. 1998;35:768–74.
23. Krishnan S, Rigby KW, O'Donnell M. Improved estimation of phase aberration profile. IEEE Trans Ultrason Ferroelectr Freq Control. 1997;44:701–13.